Biogeosciences
Open Access
Discussions

Biologically labile photoproducts from riverine non-labile dissolved organic carbon in the coastal waters

V. Kasurinen[1,2], H. Aarnos[3], and A. Vähätalo[4]

[1]University of Helsinki, Department of Forest Sciences, P.O. Box 27, Helsinki, Finland
[2]Norwegian University of Science and Technology, 7491 Trondheim, Norway
[3]University of Helsinki, Department of Environmental Sciences, P.O. Box 65, 00014 Helsinki, Finland
[4]University of Jyväskylä, Department of Bio and Environmental Sciences, P.O. Box 35, 40014, Jyväskylä, Finland

Correspondence to: V. Kasurinen (ville.kasurinen@helsinki.fi)

Discussion Paper | Discussion Paper | Discussion Paper | Discussion Paper

BGD

12, 8199–8234, 2015

BLPs from riverine non-labile DOC

V. Kasurinen et al.

Title Page

Abstract	Introduction
Conclusions	References
Tables	Figures

Back | Close

Full Screen / Esc

Printer-friendly Version

Interactive Discussion

Abstract

In order to assess the production of biologically labile photoproducts (BLPs) from non-labile riverine dissolved organic carbon (DOC), we collected water samples from ten major rivers, removed labile DOC and mixed the residual non-labile DOC with artificial seawater for microbial and photochemical experiments. Bacteria grew on non-labile DOC with a growth efficiency of 11.5 % (mean; range from 3.6 to 15.3 %). Simulated solar radiation transformed a part of non-labile DOC into BLPs, which stimulated bacterial respiration and production, but did not change bacterial growth efficiency (BGE) compared to the non-irradiated dark controls. In the irradiated water samples, the amount of BLPs stimulating bacterial production depended on the photochemical bleaching of chromophoric dissolved organic matter (CDOM). The apparent quantum yields for BLPs supporting bacterial production ranged from 9.5 to 76 (mean 39) (μmol C mol photons^{-1}) at 330 nm. The corresponding values for BLPs supporting bacterial respiration ranged from 57 to 1204 (mean 320) (μmol C mol photons^{-1}). According to the calculations based on spectral apparent quantum yields and local solar radiation, the annual production of BLPs ranged from 21 (St. Lawrence) to 584 (Yangtze) mmol C m^{-2} yr^{-1} in the plumes of the examined rivers. Complete photobleaching of riverine CDOM in the coastal ocean was estimated to produce 10.7 Mt C BLPs yr^{-1} from the rivers examined in this study and globally 38 Mt yr^{-1} (15 % of riverine DOC flux from all rivers), which support 4.1 Mt yr^{-1} of bacterial production and 33.9 Mt yr^{-1} bacterial respiration.

1 Introduction

Rivers transport 246 Mt C yr^{-1} of dissolved organic carbon to the ocean Cai (2011). A part (19 ± 16 %) (Søndergaard and Middelboe, 1995) of this terrestrial DOC is biologically labile and quickly consumed by heterotrophic bacteria in the coastal waters (Lønborg et al., 2009; Lønborg and Álvarez Salgado, 2012). The remaining majority

V. Kasurinen et al.

(81 ± 16 %) of terrestrial DOC (tDOC) is biologically non-labile (Søndergaard and Middelboe, 1995). In the coastal waters, the primary sinks for non-labile DOC are slow microbial metabolism or photochemical transformations (Bauer et al., 2013). Photochemical reactions can transform non-labile tDOC to dissolved inorganic carbon (DIC) or biologically labile photoproducts (BLPs), the latter being rapidly assimilated by microbes (Wetzel et al., 1995). The assimilation of non-labile tDOC (directly or after photochemical transformation) contributes to heterotrophy of coastal waters (Smith and Hollibaugh, 1993) and couples tDOC to marine food webs (Vähätalo and Järvinen, 2007; Vähätalo et al., 2011). The extent of this coupling depends also on the fraction of assimilated tDOC converted to bacterial biomass (i.e., bacterial growth efficiency, BGE) (del Giorgio and Cole, 1998; del Giorgio and Davis, 2003).

By operational definition, BLPs are compounds produced by photochemical reactions and transformed into a more labile form than the original compounds in DOC. The amount of BLPs is typically quantified experimentally as bacterial respiration, bacterial production or associated loss of DOC (= bacterial carbon demand) in irradiated DOC in excess of that found in non-irradiated dark control DOC (Wetzel et al., 1995; Smith and Benner, 2005). In order to translate the experimental findings to environmental processes, the amounts of BLPs have been related to the number of photons absorbed by chromophoric dissolved organic matter (CDOM) yielding to an apparent quantum yield (AQY) for production of BLPs (Miller et al., 2002; Vähätalo et al., 2011; Aarnos et al., 2012; Reader and Miller, 2014; Cory et al., 2014).

The production of BLPs is also linearly related to the photochemical loss of CDOM (photobleaching) (Kieber et al., 1990; Miller and Moran, 1997; Bertilsson and Tranvik, 2000; Obernosterer and Herndl, 2000; Brinkmann et al., 2003). Although, this quantitative relationship between the production of BLPs and photobleaching could be also used to estimate the photoproduction of BLPs in the surface waters, it has to our knowledge never been used for such a purpose. Bacterial production on BLPs can support both heterotrophic food webs and primary production in the coastal waters (Vähätalo and Järvinen, 2007; Vähätalo et al., 2011). The bacterial production on BLPs depends

in part on BGE on BLPs. Irradiation of DOC can decrease (15 studies) or increase BGE (5 studies) compared to non-irradiated DOC (reviewed by Abboudi et al. (2008)). Despite of these comparisons, between irradiated and non-irradiated DOC, the BGE on BLPs has not been determined and our study provides the first BGE estimate on BLPs.

This study estimates the production of BLPs from non-labile tDOC in the coastal waters and determines BGE on BLPs. We collected water samples from ten large rivers that produce together 28 % of tDOC flux to the ocean and aged the samples with indigenous microbes for the removal of labile DOC. The remaining non-labile DOC was mixed (1 : 1) with artificial seawater to simulate chemical matrix of coastal ocean. The sterile filtered mixtures of non-labile DOC and seawater were irradiated with simulated solar radiation. The irradiated waters received indigenous bacteria and the amount of BLPs was measured separately as bacterial production (BP on BLPs) and respiration (BR on BLPs) in excess of that found in the non-irradiated dark control waters. The BP or BR on BLPs was related to the number of absorbed photons for the calculation of AQY and also to the photobleaching (BLPs vs. photobleaching approach). The annual production of BP on BLPs and BR on BLPs ($\mathrm{mol\,C\,m^{-2}\,yr^{-1}}$) in the river plumes was calculated from AQYs and the annual solar radiation in the coastal ocean in the front of each river. We calculated the annual production of BLPs from the annual CDOM fluxes for each river ($\mathrm{Mt\,C\,yr^{-1}}$ per river) using the BLPs vs. photobleaching approach and assuming that photobleaching of tDOM in the coastal ocean equals the annual tDOM flux. As the rivers examined contribute 28 % of tDOC flux to the ocean, we dared to extrapolate our finding to global scale simply by assuming that the rivers examined here are representative for the remaining 72 % of tDOC flux by other rivers.

BLPs from riverine non-labile DOC

V. Kasurinen et al.

Back | Close

Full Screen / Esc

Printer-friendly Version

Interactive Discussion

Discussion Paper | Discussion Paper | Discussion Paper | Discussion Paper

2 Material and methods

2.1 Material

The rivers selected for this study (Table 1) drain 25 % of the land area, contribute 28 % to the global tDOC flux, and 33 % to the freshwater discharge to the ocean (Carlson, 2002; Cauwet, 2002; Coynel et al., 2005; Milliman and Farnsworth, 2011). For the collection of water samples, empty polyethylene containers (cleaned with detergent, rinsed with HCl and finally copiously rinsed with ion exchanged water; MQ) were shipped to the local collaborators at ten major rivers (see acknowledgments). The containers were filled in the center of the stream by direct immersion below the surface, except for the Mississippi and St. Lawrence Rivers where water about 3 m below the surface was collected with Niskin bottles. The samples collected for this study has been used earlier for the determination of dissolved black carbon (Jaffé et al., 2013), dissolved iron (Xiao et al., 2013) and the photochemical isotopic fractionation of DOC (Lalonde et al., 2014).

Artificial seawater was prepared according to Kester et al. (1967) by dissolving pro analysis grade of inorganic salts (VWR International) to MQ water. Prior to use, glassware and quartzware were washed in a dishwasher, rinsed out with 7 % HCl and MQ water, and combusted for several hours (450 °C).

2.2 Experimental

2.2.1 Sample preparation

In order to remove labile DOC, the collected water samples were not filtered or preserved, but kept in darkness and sent to our laboratory in Helsinki, Finland by air cargo. The median transport time between the sampling and the arrival to Helsinki was 33 days (Table 1). Upon arrival to the laboratory, the water samples were filtered through 1 µm filters (quick rinsed membrane cartridge, Nuclepore or double layer of

BLPs from riverine non-labile DOC

V. Kasurinen et al.

BLPs from riverine non-labile DOC

V. Kasurinen et al.

Printer-friendly Version

Interactive Discussion

track-etch polyester membrane filter cartridge, Graver Technologies) and stored in the dark at +4 °C. We assume that the microbes present in the water samples consumed the labile DOC during the transportation, which allowed us to carry out the experimental work with non-labile DOC. The amount of labile DOC from the St. Lawrence river sample was $19 \pm 1\,\%$ ($n = 3$) in the St. Lawrence River sample (Lalonde et al., 2014), which is in agreement with the proportion of labile riverine DOC being $19 \pm 16\,\%$ (Søndergaard and Middelboe, 1995; Lønborg and Álvarez Salgado, 2012; Asmala et al., 2014).

Our salinity adjustment followed by filtration mimics a potential removal of iron via flocculation and related loss in photochemical reactivity and is expected to result a matrix characteristic for photochemical transformation of non-labile tDOC in the coastal waters 2.2.1. In order to assess BGEs and the production of BLPs from non-labile tDOC under conditions representing coastal waters, the 1 µm-filtered river water samples were mixed 1 : 1 with artificial seawater. In the mixtures, the ionic composition was similar to that of seawater but the salinity (16) was half of that found in the ocean. For abiotic photochemical experiments, the 1 µm filtered river water samples mixed with artificial seawater were further aseptically filtered through 0.2 µm membrane filters (Palls Supor 200) into 170 mL glass or quartz flasks to be closed with ground-glass stoppers without headspace.

2.2.2 Irradiations

The quartz flasks were irradiated for 44 to 46 h with $765\,\mathrm{W\,m^{-2}}$ simulated solar radiation (Atlas Suntest CPS+ solar simulator) in a MQ-water bath regulated to 20 °C with a Lauda RE-112 thermostat like in our earlier study (Aarnos et al., 2012). The glass flasks wrapped into aluminum foil were kept in the same water bath (dark controls) or at 4 °C (initials).

2.2.3 Bioassays

For the bioassays, the irradiated and the dark control samples from each river received a 10 % (vol/vol) inoculum of bacterioplankton prepared from their corresponding river by passing the 1 µm-filtered river water through GF/F filters (nominal pore size of 0.7 µm, Whatman) for the removal of the grazers of bacterioplankton. The bioassay samples received NH_4Cl and KH_2PO_4 to the final concentrations of $1.2\,mg\,N\,L^{-1}$ and $0.13\,mg\,P\,L^{-1}$, respectively, and were divided into two aliquots for the determination of bacterial respiration (BR) or bacterial production (BP).

2.2.4 Bacterial respiration

BR was determined as a consumption of dissolved oxygen (O_2) measured with needle-type oxygen microsensor optodes (PreSens GmbH, Regenburg, NTH-PSt1-L5-TF-NS40) (Warkentin et al., 2007, 2011) at 15 min intervals from aliquots closed in biological oxygen demand bottles incubated in darkness in a water bath at 20 °C (Lauda RE-112 thermostat). An optode was inserted into the sample via a hole drilled through the ground-glass stopper and sealed with parafilm. The drift of instrument defining the detection limit for BR was measured in three blank experiments, where MQ water was incubated for 300 h under conditions identical to respiration measurements. During the blank experiments, the apparent decline of O_2 was $1.5 \pm 0.5\,\mu mol\,L^{-1}\,300\,h^{-1}$ (mean $\pm$ sd, $n = 3$). The decline in the concentration of O_2 was converted into an increase in the concentration of CO_2 assuming $1:1$ molar ratio between the consumed O_2 and the produced CO_2 in BR. The selected respiratory quotient makes our study comparable to earlier studies, which have used values ranging from 0.82 to 1.2 (Søndergaard and Middelboe, 1995; del Giorgio et al., 1997; del Giorgio and Cole, 1998; Cory et al., 2014). The temporal trend of accumulated CO_2 was determined by a polynomial fitting to the measurements with the smooth spline function in R software (R Core Team, 2014).

2.2.5 Bacterial production

To determine bacterial production (BP), 10 mL samples were preserved with formaldehyde (final concentration 5 %) daily from aliquots incubated in dark conditions at room temperature (mean 22 °C, range from 20 to 24 °C) with an air-head space. The bacterial cells from the preserved samples were filtered on 0.2 μm polycarbonate filters (GE water & Process Technologies) and stained with acridine orange (Hobbie et al., 1977). Bacterial densities were estimated from cell counts from $\geq$ 20 fields with an epifluorescence microscope (Aristoplan). The cell volumes were determined by digital image analysis (Image Analysis & LabMicrobe software; Massana et al.1997). The volumes of cells were converted to carbon using a conversion factor of $0.12\,\mathrm{pg\,C}\,(\mu m^3)^{0.7}$ and the total carbon-biomass of bacterioplankton assemblage was calculated by multiplying the organic carbon content of cells with the density of cells (Norland, 1993).

2.2.6 Defining BLPs and BGEs

For the bacteria growing in the irradiated sample, the response to BLPs was considered to be largest in the end of logarithmic growth phase defined as the first day with maximum biomass during the 12 day-long bioassay (Stepanauskas et al., 2002). On that day (varying from 5 to 12 days), the difference in the accumulated BP or BR between the dark control and the irradiated samples represented the BP or BR on BLPs. The bacterial growth efficiency (BGE) was calculated as BP/(BP + BR).

2.3 Analytical measurements

The absorbance by CDOM was measured with a spectrophotometer (Shimadzu UV 2550) in triplicates against MQ water reference using a 0.05 m quartz cuvette. The absorbance by CDOM was converted into an absorption coefficient ($a_{\mathrm{CDOM},\lambda}$) accounting for the path length of the cuvette and transforming the 10-base logarithm to a Naperian-based logarithm (ln(10)).

2.4 The apparent quantum yields for the production of BLPs

Spectral apparent quantum yields (AQYs) for the production of BLPs supporting bacterial production (BP) or bacterial respiration (BR) ($AQY_{BP,\lambda}$ or $AQY_{BP,\lambda}$) were calculated as:

$$AQY_{BP,\lambda} \text{ or } AQY_{BR,\lambda} = \frac{BP \text{ or } BR}{\text{photons absorbed by CDOM}(\lambda)} \tag{1}$$

where BP or BR on BLPs are the bacterial production or respiration based on BLPs (mol C) and photons absorbed represents the spectrally resolved absorption of photons by CDOM during the irradiation experiment (mol photons at the spectral range from 290 to 750 nm) and λ specific wavelength. The latter was calculated by accounting for the spectral dose of photons, the optical path length, and the absorption characteristics of samples as explained in our earlier study (Aarnos et al., 2012). $AQY_{BP,\lambda}$ and $AQY_{BR,\lambda}$ were assumed to depend on wavelength according to:

$$AQY_\lambda = c d^{-d\lambda} \tag{2}$$

where AQY_λ is $AQY_{BP,\lambda}$ or $AQY_{BR,\lambda}$, c (mol C mol photons^{-1}) and d (nm^{-1}) are positive constants, and λ is the wavelength (nm). The parameters c and d in Eq. (2) were iterated from Eq. (1) by unconstrained nonlinear optimization (the "fminsearch" function of the Matlab 7.9.0) as in our earlier publications (Vähätalo et al., 2011; Aarnos et al., 2012).

2.5 The production of BLPs based on AQYs

The measured $AQY_{BP,\lambda}$ or $AQY_{BR,\lambda}$ was used to calculate the production rate of BLPs in the river plumes according to:

$$pr = \int_{\lambda_{min}}^{\lambda_{max}} AQY_\lambda Q_\lambda (a_{CDOM,\lambda} a_{tot,\lambda}^{-1}) d\lambda \tag{3}$$

Full Screen / Esc

Printer-friendly Version

Interactive Discussion

where pr is the production rate of BLPs supporting BP or BR over the entire water column (mol C m^{-2} yr^{-1}), AQY$_\lambda$ is AQY$_{BP,\lambda}$ or AQY$_{BR,\lambda}$, Q$_\lambda$ represents the spectrum of solar radiation absorbed by the entire water column (mol photons m^{-2} yr^{-1} nm^{-1}), and the ratio $a_{CDOM,\lambda} a_{tot,\lambda}^{-1}$ (dimensionless) is the contribution of tDOC to the total absorption coefficient $a_{tot,\lambda}$ (m^{-1} nm^{-1}) (Aarnos et al., 2012). The integration was done from λ_{min} of 290 nm to λ_{max} of 750 nm. Q_λ was calculated as the product of a standard solar radiation spectrum (ASTM G173-03; Chu and Liu, 2009) normalized with global radiation and the annual mean global radiation determined for the area of each river plume examined. The latter was calculated from monthly values over the years 1984 to 2000 (Hatzianastassiou et al., 2005). Terrestrial CDOM was assumed to absorb all photolytic photons ($a_{CDOM,\lambda} a_{tot,\lambda}^{-1} = 1$; Eq. 3). Therefore the calculated rates apply for those coastal regions, where tCDOM from rivers dominates the absorption of photolytic solar radiation (e.g. river plumes).

2.6 The production of BLPs based on photobleaching

The annual production of BLPs from tCDOM in the coastal ocean was estimated from the measured relationship between BLPs and photobleaching. The latter was assumed to be the only sink for tCDOM discharged by rivers to coastal ocean (Nelson and Siegel, 2013). In this case, the amount of photobleached tCDOM equals the CDOM flux by the rivers. The annual CDOM fluxes for Lena, Mississippi and St. Lawrence rivers were taken from the literature (Stedmon et al., 2011; Spencer et al., 2013) and converted to $a_{CDOM,300}$ flux with spectral slope coefficients (Stedmon et al. (2011); 17.6 and 16.3 µm^{-1}) measured for Mississippi and St. Lawrence CDOM, respectively. In the absence of published fluxes for the remaining rivers, the annual CDOM fluxes were estimated by multiplying the measured $a_{CDOM,300}$ with the annual water discharge (Cauwet, 2002; Coynel et al., 2005). The production of BLPs supporting BP by each river (mol C yr^{-1}) was calculated by multiplying the CDOM flux of each river (m^2 yr^{-1}) with the relationship (mol C m^{-2}) between the BP on BLPs and photobleaching of

CDOM at 300 nm. The BR on BLPs was calculated from the mean BGE on BLPs (BR = BP/BGE – BP). Finally, the total production of BLPs (mol C yr^{-1}) was obtained as a sum of BR and BP on BLPs.

2.7 Statistical analysis

⁵ Statistical differences between the samples were tested with two-tailed paired t tests (heteroscedastic) by comparing observed response between the irradiated and the dark control samples. All statistical analyses were carried out by using R language and a significance level of 0.05 (R Core Team, 2014). We used linear regression to evaluate the dependency between photobleaching and and BP or BLPs.

¹⁰ # 3 Results

3.1 Photobleaching of riverine CDOM in a seawater matrix

When 0.2 µm filtered river waters without labile DOC (Table 1) were mixed with artificial seawater and irradiated, the simulated solar radiation photobleached CDOM at 300 nm ($a_{CDOM,300}$) by 50.4 ± 2.6 % (mean ± sd here and elsewhere in the results; Ta-
¹⁵ ble 2). The amount of photobleaching expressed as absorption coefficient ranged from 0.48 ± 0.06 m^{-1} (Ganges–Brahmaputra) to 12.42 ± 0.06 m^{-1} (Congo) when calculated as the difference in $a_{CDOM,300}$ between the dark control and the irradiated samples ($\Delta a_{CDOM,300}$, Table 2).

3.2 Bacterial production

²⁰ In order to assess bacterial production (BP) on the irradiated and the dark control non-labile DOC, we introduced an inoculum of riverine bacterioplankton to the irradiated and the dark control samples resulting in the bacterial cell densities from 0.006 to 0.240 × 10^9 cells L^{-1} (t = 0 in Table 3). The bacteria increased their densities by one to

two orders of magnitude in five to 12 days (Table 3) in the irradiated samples and 33 to 152 % higher more than in the dark control samples (Table 3).

The bacterial cell densities were converted to biomasses by accounting for the bacterial cell volumes, which were not different between the dark control and the irradiated samples (paired t test, df = 9, $p > 0.05$). In the dark controls, the accumulated BP ranged from 0.5 ± 0.1 (Lena) to 3.9 ± 0.2 (Congo) $\mu mol\,C\,L^{-1}$ (Fig. 1). BP was higher in the irradiated than in the dark control samples (paired t test, df = 9, $p = 0.003$) and ranged from 1.2 ± 0.1 (Lena) to 8.7 ± 0.6 (Congo) $\mu mol\,C\,L^{-1}$ (Fig. 1). BP on BLPs, calculated as the difference between the irradiated and the dark control samples, ranged from 0.6 ± 0.3 (Ganges–Brahmaputra) to 4.8 ± 0.8 (Congo) $\mu mol\,C\,L^{-1}$ (Fig. 1). The BP on BLPs was significantly related to the photobleaching by a linear regression coefficient of $0.336\,mmol\,C\,L\,m^{-2}$ (Fig. 2).

3.3 Bacterial respiration

In the dark controls, bacterial respiration (BR) accumulated usually linearly with time indicating relatively constant rates of respiration throughout the bioassay (Fig. 3). In the irradiated samples, the kinetics of BR was different and rates typically higher than in the dark control samples (Fig. 3). The BR on BLPs (Fig. 4) was calculated from the difference in respiration between the irradiated and dark control samples (Fig. 3). After a lag-phase, BR on BLPs typically accumulated rapidly, but leveled off at the late phase of bioassay (Fig. 4). The BR on BLPs accumulated by the time of maximum biomass was undetectable ($-1.4 \pm 1.39\,\mu mol\,C\,L^{-1}$) with Ganges–Brahmaputra BLPs and highest ($27.8 \pm 1.33\,\mu mol\,C\,L^{-1}$) with Yangtze BLPs (Fig. 4).

3.4 Bacterial growth efficiency

When BGE was calculated from the biomass (Fig. 1) and the respiration gained by the time of maximum biomass (Figs. 3 and 4), it was lowest 3.0 % and highest 27.7 % in the irradiated DOC from Yangtze and Ganges–Brahmaputra, respectively, while in the

dark controls BGE ranged from 3.6 % (Yangtze) to 15.3 % (Amazon) (Table 4). BGE on BLPs ranged from 2.8 % (Yangtze) to 21.5 % (Amazon) (Table 4). The mean BGEs were not different among the irradiated DOC, the dark control DOC or BLPs (paired t test, df = 7, $p > 0.05$) (Table 4).

3.5 Apparent quantum yields and production rates of BLPs

When the BP on BLPs (Fig. 1) was divided by the spectrum of photons absorbed during the irradiation, the spectral AQY for the production of BLPs supporting BP ($AQY_{BP,\lambda}$; Eq. 2) was defined by the parameters c and d shown in Table 5. Based on these parameters, the calculated AQY_{BP} ranged from 9.5 to 76 with median of µmol C mol photons^{-1} at 330 nm, a wavelength of solar radiation responsible for highest production of BLPs (Table 5) (Miller et al., 2002; Vähätalo et al., 2011; Aarnos et al., 2012). The corresponding values for the production of BLPs supporting BR ($AQY_{BR,330}$) ranged from 57 to 1203 with median of 186 µmol C mol photons^{-1} (Table 5).

In the river plumes, the annual production of BLPs supporting BP ranged from 1.0 (Lena) to 33 mmol C m^2 yr^{-1} (Ganges–Brahmaputra) (Table 6) when calculated (Eq. 3) with $AQY_{BP,\lambda}$ (Table 5) and the local annual mean solar irradiance in the coastal ocean at the front of each river. The corresponding production of BLPs supporting BR ranged from 19 (St. Lawrence) to 574 mmol C m^{-2} yr^{-1} (Yangtze) (Table 6). The total production of BLPs ranged from 21 (St Lawrence) to 584 mmol C m^{-2} yr^{-1} (Yangtze) when calculated as the sum of BLPs supporting BP and BR (Table 6).

3.5.1 An estimate for the global production of BLPs

The relationship between BP on BLPs and $\Delta a_{CDOM,300}$ (Fig. 2) was multiplied with the annual CDOM fluxes (Table 7) to estimate the photobleaching of CDOM and related production of BLPs from non-labile tDOC of each river in the coastal ocean. The photobleaching of CDOM fluxes was calculated to promote altogether 1.1 ± 0.3 Mt C yr^{-1} BP on BLPs (mean ± 95 % confidence interval; Table 7). The corresponding amount of

BR on BLPs was calculated to be $9.5 \pm 4.8\,\mathrm{MtC\,yr^{-1}}$ when accounting for the 12.0 % BGE on BLPs (Table 7). The sum of BP and BR on BLPs was $10.7 \pm 4.5\,\mathrm{MtC\,yr^{-1}}$ representing the total production of BLPs (Table 7). This total production of BLPs corresponds to 15 ± 6.8 % of the total DOC flux ($69\,\mathrm{MtC\,yr^{-1}}$) of examined rivers (Table 7).

Assuming that the rivers examined responsible for 28 % of global DOC flux are representative for the remaining 72 % DOC flux to ocean, the estimate for the global coastal production of BLPs from tDOC is $38.0 \pm 15.9\,\mathrm{MtC\,yr^{-1}}$ supporting $4.1 \pm 1.1\,\mathrm{MtC\,yr^{-1}}$ BP and $33.9 \pm 16.9\,\mathrm{MtC\,yr^{-1}}$ BR.

4 Discussion

4.1 Global fluxes of BLPs from terrestrial DOC

Our study provides the first estimate for the production of BLPs from tDOC in the coastal waters in the front of ten major rivers across five continents. The BLPs from tDOC ($38.0 \pm 15.9\,\mathrm{MtC\,yr^{-1}}$; this study) contribute little to the production of BLPs in global coastal water estimated earlier ($206\,\mathrm{MtC\,yr^{-1}}$) (Miller et al., 2002). That estimate is nearly as large as global riverine DOC flux to the ocean ($246\,\mathrm{MtC\,yr^{-1}}$) (Cai, 2011). There much of the earlier estimate must be based on the autochthonous production in marine waters and tells little about the coupling of tDOC to marine waters trough the microbial loop.

The annual production of BLPs from tDOC in coastal waters ($38.0 \pm 15.9\,\mathrm{MtC\,yr^{-1}}$) estimated in this study is larger than the global photochemical production of dissolved inorganic carbon (DIC) in inland waters (Koehler et al., 2014). This comparison indicates that although solar radiation transforms a remarkable amount of DOC in lakes and rivers, the majority of photochemical processing of terrestrial and freshwater DOC takes place in coastal waters.

According to the present study, the BGE on BLPs is 12 % and thus the majority of assimilated BLPs will be quickly respired to DIC totaling $33.9 \pm 16.9\,\mathrm{MtC\,yr^{-1}}$ in the global

coastal waters. This amount provides an additional source of DIC to coastal ocean in addition to the riverine flux of DIC ($407\,\mathrm{Mt\,C\,yr^{-1}}$; Cai, 2011). This study estimates that BLPs from tDOC support $4.1 \pm 1.1\,\mathrm{Mt\,C\,yr^{-1}}$ of BP in the global coastal waters. This BP is not alone a source of carbon to food webs, but is associated with N and P bound in bacterial biomass (Smith and Benner, 2005; Vähätalo et al., 2011). Assuming stoichiometric amounts of N and P associated to bacterial biomass (mass C : N : P ratio of 17 : 4 : 1) (Goldman et al., 1987), the assimilation of BLPs from terrestrial tDOC transfers $4.5\,\mathrm{Mt\,C\,yr^{-1}}$, $1.06\,\mathrm{Mt\,N\,yr^{-1}}$ and $0.26\,\mathrm{Mt\,P\,yr^{-1}}$ to the coastal food webs through the grazers of bacterioplankton.

4.1.1 BLPs, photobleaching and CDOM fluxes

In this study, the production of BLPs is related to the photobleaching of CDOM with a R^2 0.88 (Fig. 2). Similar relationships has been found also in earlier studies (Miller and Moran, 1997; Obernosterer and Herndl, 2000; Brinkmann et al., 2003). For example, $\Delta a_{\mathrm{CDOM},300}$ explains extremely well ($R^2 > 96\,\%$) of the photoproduction of three individual BLP-compounds: formaldehyde, acetaldehyde and glyoxylate (Kieber et al., 1990). The corresponding R^2 is lower (0.67) for the relationship between a group of BPLs (carboxylic acids) and $\Delta a_{\mathrm{CDOM},365}$ determined for 38 Swedish lakes (Bertilsson and Tranvik, 2000). Our R^2-value (Fig. 2) is higher than the corresponding one for 38 lake water samples (Bertilsson and Tranvik, 2000). This is at first glance surprising since our DOC was collected from ten global rivers covering a wide climatic range and land use not limited for a small region (Sweden) as in an earlier study (Bertilsson and Tranvik, 2000). The relatively high R^2-values in this study may be explained in part by the same chemical matrix (artificial coastal water) used in our experiments. Additionally, the rivers examined here integrate the variability of DOM across their large catchments. For example, one third of 7838 different chemical compounds assigned by ultrahigh-resolution mass spectral analysis to the water samples examined in this study were shared among all river samples (Wagner et al., 2015). A conclusion from

this and many other studies (Kieber et al., 1990; Miller and Moran, 1997; Bertilsson and Tranvik, 2000; Obernosterer and Herndl, 2000; Brinkmann et al., 2003) is that the production of BLPs is quantitatively linked the photobleaching of CDOM, which makes it as a useful proxy for the production of BLPs.

Our estimate for the global production of BLPs from terrestrial DOM bases on an assumption that the riverine CDOM flux will be photobleached completely in the coastal ocean. We used published CDOM fluxes for Mississippi, St. Lawrence and Lena Rivers (Stedmon et al., 2011; Spencer et al., 2013), but for the remaining rivers the CDOM flux was estimated simply by multiplying the measured CDOM with the published water discharge (Table 7). This method provides only rough estimates for CDOM fluxes and causes uncertainty also for our global estimates of BLPs. Therefore an additional data on riverine CDOM fluxes in the future will improve our estimate for CDOM fluxes and related production of BLPs. The majority of global riverine CDOM flux enters to the mixing layer of coastal waters, where solar radiation photobleaches CDOM efficiently and leaves not traces of terrestrial CDOM to be found in the surface of open ocean (review by Nelson and Siegel (2013) and references therein). Our assumption for complete photobleaching may not hold entirely for the rivers (such as Lena in this study) discharging to Arctic Ocean, which transfers $78\,200\,\mathrm{Gm}^2\,\mathrm{yr}-1$ of riverine CDOM to North Atlantic (calculated for 300 nm from the slope and flux estimated by Granskog et al., 2012). A part of this CDOM flux is directed to the deep ocean without photobleaching as a part of deep water formation in the North Atlantic (Nelson and Siegel, 2013). Thus our assumption for complete photobleaching is relatively well but not entirely supported by our current estimate for photobleaching being the major sink for riverine CDOM in the coastal ocean.

4.1.2 AQYs for BLPs

Our $AQY_{BP,330}$s (9.5–76 $\mu\mathrm{mol\,C\,mol\,photons}^{-1}$ Table 5) overlap the range of $AQY_{BP,330}$ in the Baltic Sea (23 to 111 $\mu\mathrm{mol\,C\,mol\,photons}^{-1}$) (Aarnos et al., 2012). Our

AQY$_{BR,330}$s (57 to 1204 (µmol C mol photons^{-1}) are generally lower than the previously reported 1391 (µmol C mol photons^{-1}) for river water and 1090 (µmol C mol photons^{-1}) for water draining a salt marsh (Miller et al., 2002), but similar to those for rivers and lakes in Alaska (Cory et al., 2014). In the earlier studies, the AQY$_{BP}$s reported by

5 Aarnos et al. (2012) are lower than AQY$_{BR}$s reported by Miller et al. (2002) and Cory et al. (2014). To the best of our knowledge, our study presents the first simultaneous determinations of AQY$_{BP}$ and AQY$_{BR}$ and shows that AQYs for bacterial respiration are larger than for bacterial production.

In this study, BLPs were consumed by riverine bacteria, which survived at the coastal

10 salinities, increased their biomass by one to two orders of magnitude and reached a detectable peak in biomass within < 12 days. The bacterial inoculum used by Miller et al. (2002) was thousand-times larger and the time of bioassay longer than in the present study. The bacteria used by Miller et al. (2002) were able to assimilate more BPLs resulting in higher AQYs than in our study. Although our bioassays for the determination

15 of BPLs lasted up to 12 days, the initial cell densities of inoculum were low and reached typical densities found in surface water not until the end of bioassay (Table 3). The BLPs determined in this study likely represent the most bioavailable fraction of BLPs (Kieber and Mopper, 1987). The number of known chemically distinct BLP-compounds was 14 in an early review (Moran and Zepp, 1997), but had increased to 44 in a later review

20 (Vähätalo, 2009). A more recent study using a high resolution of mass spectrometry identified 1835 chemical formulae that were produced by solar radiation-induced photochemical reactions (Rossel et al., 2013).From these formulae 44 % were not observed in a treatment with high microbial activity indicating that the number of BLP-compounds was 807 and that BLPs represent a diverse group of compounds (Rossel et al., 2013).

25 Although, by a definition BLPs are biologically more labile than the original DOC, the biodegradability of individual BLP-compounds likely varies and may form a continuum like with the bulk DOM (Moran and Zepp, 1997; Vähätalo, 2009; Vähätalo et al., 2010; Rossel et al., 2013). Thus, as the present study refers to the most bioavailable fraction of BLPs, the entire pool of BPLs is likely larger than what was measured in this study.

Full Screen / Esc

Printer-friendly Version

Interactive Discussion

4.1.3 BGEs on BLPs and non-labile DOC

Our BGE on BLPs (12.0 ± 7.2 %; Table 4) provides the first direct estimate for the BGE of microbial communities on a group of compounds classified as BLPs. Our values can be compared to BGEs reported for single compounds such as acetic and formic acids (Bertilsson and Tranvik, 1998). BGEs on formic and acetic acids has been 2 and 41 %, in one study (Bertilsson and Tranvik, 1998), but 20–27 and 73–80 %, respectively, in another study (Remington et al., 2011). The earlier studies demonstrate that BGE on a single BLP compound can vary and thus it is a challenge to determine BGE separately for each BLP compound and compile them together for an overall BGE on all BLPs. Such a simple overall BGE (12.0 ± 7.2 %) can now be applied on BLPs based on the results of the present study.

Our BGE on DOM in the dark controls (11.5 ± 3.9 %, Table 4) represents an estimate for BGE on non-labile tDOC in coastal waters. This estimate falls to the lower range of hundreds BGE determinations done with freshly collected water representing BGEs primarily on labile DOC (Kroer, 1993; del Giorgio and Cole, 1998; Wikner et al., 1999). Our BGE on non-labile DOC is similar to BGE (mean 11 %) on riverine DOC aged for 100 to 450 days (Asmala et al., 2014). An extensive aging of humic lake water by 6 years resulted in BGEs of 5–6 % (Kragh et al., 2008). The results of this (Figs. 1 and 3; Tables 3 and 4) and earlier studies (Kragh et al., 2008; Berggren et al., 2009; Vähätalo et al., 2010; Asmala et al., 2014) emphasize that bacteria can assimilate non-labile tDOC, but a relatively low BGE.

5 Conclusions

Our study shows that the mineralization and transformation of tDOC will continue in the coastal ocean after the quick consumption of labile tDOC at estuaries (Figs. 1–3, Tables 3 and 4). As the tDOC is transported towards open ocean, the microbes will continue to assimilate non-labile DOC with BGEs around 11.5 % (Table 4; Asmala

et al., 2014). The photochemical transformation of tDOC is expected to increase after the turbidity maximum, advection and mixing into optically transparent marine waters. These reactions transform tDOC directly into CO_2 Miller and Zepp (1995); Aarnos et al. (2012) and into BLPs to be assimilated by bacteria with BGEs around 12 % (Table 4). The photochemical production of BLPs in coastal waters can be estimated with two approaches. The AQYs can estimate the production of BLPs locally in the rivers plumes at any specified time with known solar irradiance (Tables 5 and 6). Similar estimates can be made by multiplying photobleaching of CDOM (Whitehead et al., 2000; Osburn et al., 2001; Vähätalo and Wetzel, 2004) with $0.335\,\mathrm{mmol\,C\,m^{-2}}$ (Fig. 2). Photobleaching also provides a robust estimate for the annual production of BLPs by each river or all rivers (Table 7). Although this estimate does not specify where and when the photochemical transformations take place, it improves integrative synthesis on the fate of tDOC in the coastal ocean and its linkages to marine food webs (Bauer et al., 2013).

References

Aarnos, H., Ylöstalo, P., and Vähätalo, A. V.: Seasonal phototransformation of dissolved organic matter to ammonium, dissolved inorganic carbon, and labile substrates supporting bacterial biomass across the Baltic Sea, J. Geophys. Res., 117, 1–14, doi:10.1029/2010JG001633, 2012. 8201, 8204, 8207, 8208, 8211, 8214, 8215, 8217

Abboudi, M., Jeffrey, W. H., Ghiglione, J.-F., Pujo-Pay, M., Oriol, L., Sempéré, R., Charrière, B., and Joux, F.: Effects of photochemical transformations of dissolved organic matter on bacterial metabolism and diversity in three contrasting coastal sites in the Northwestern Mediterranean Sea during summer, Microb. Ecol., 55, 344–57, doi:10.1007/s00248-007-9280-8, 2008. 8202

Asmala, E., Autio, R., Kaartokallio, H., Stedmon, C. A., and Thomas, D. N.: Processing of humic-rich riverine dissolved organic matter by estuarine bacteria: effects of predegradation and inorganic nutrients, Aquat. Sci., 76, 451–463,, doi:10.1007/s00027-014-0346-7, 2014. 8204, 8216

Bauer, J. E., Cai, W.-J., Raymond, P. A., Bianchi, T. S., Hopkinson, C. S., and Regnier, P. A. G.: The changing carbon cycle of the coastal ocean, Nature, 504, 61–70, doi:10.1038/nature12857, 2013. 8201, 8217

Berggren, M., Laudon, H., and Jansson, M.: Aging of allochthonous organic carbon regulates bacterial production in unproductive boreal lakes, Limnol. Oceanogr., 54, 1333–1342, doi:10.4319/lo.2009.54.4.1333, 2009. 8216

Bertilsson, S. and Tranvik, L.: Photochemical transformation of dissolved organic matter in lakes, Limnol. Oceanogr., 45, 753–762, doi:10.4319/lo.2000.45.4.0753, 2000. 8201, 8213, 8214

Bertilsson, S. and Tranvik, L. J.: Photochemically produced carboxylic acids as substrates for freshwater bacterioplankton, Limnol. Oceanogr., 43, 885–895, 1998. 8216

Brinkmann, T., Hörsch, P., Sartorius, D., and Frimmel, F. H.: Photoformation of low-molecular-weight organic acids from brown water dissolved organic matter, Environ. Sci. Technol., 37, 4190–4198, doi:10.1021/es0263339, 2003. 8201, 8213, 8214

Cai, W.-J.: Estuarine and coastal ocean carbon paradox: CO_2 sinks or sites of terrestrial carbon incineration?, Ann. Rev. Mar. Sci., 3, 123–145, doi:10.1146/annurev-marine-120709-142723, 2011. 8200, 8212, 8213

Carlson, C. A.: Production and Removal Processes, in: Biogeochemistry of Marine Dissolved Organic Matter, edited by: Hansell, D. A. and Carlson, C. A., 91–151, Elsevier, 2002. 8203

Cauwet, G.: DOM in the Coastal Zone, in: Biogeochemistry of Marine Dissolved Organic Matter, edited by: Hansell, D. A. and Carlson, C. A., 579–609, Academic Press, San Diego, 2002. 8203, 8208, 8230

Chu, S. and Liu, L.: Analysis of terrestrial solar radiation exergy, Sol. Energy, 83, 1390–1404, doi:10.1016/j.solener.2009.03.011, 2009. 8208

Title Page

Abstract | Introduction

Conclusions | References

Tables | Figures

|◀ | ▶|

◀ | ▶

Back | Close

Full Screen / Esc

Printer-friendly Version

Interactive Discussion

Cory, R. M., Ward, C. P., Crump, B. C., and Kling, G. W.: Sunlight controls water column processing of carbon in arctic fresh waters, Science, 345, 925–928, doi:10.1126/science.1253119, 2014. 8201, 8205, 8215

Coynel, A., Seyler, P., Etcheber, H., Meybeck, M., and Orange, D.: Spatial and seasonal dynamics of total suspended sediment and organic carbon species in the Congo River, Global Biogeochem. Cy., 19, 1–17, doi:10.1029/2004GB002335, 2005. 8203, 8208, 8230

del Giorgio, P. A. and Cole, J. J.: Bacterial growth efficiency in natural aquatic systems, Annu. Rev. Ecol. Syst., 29, 503–541, doi:10.1146/annurev.ecolsys.29.1.503, 1998. 8201, 8205, 8216

del Giorgio, P. A. and Davis, J.: 17 – patterns in dissolved organic matter lability and consumption across aquatic ecosystems, in: Aquatic Ecosystems, a volume in Aquatic Ecology, edited by: Findlay, S. E. G. and Sinsabaugh, R. L., Academic Press, Burlington, doi:10.1016/B978-012256371-3/50018-4, 399–424, 2003. 8201

del Giorgio, P. A., Cole, J. J., and Cimbleris, A.: Respiration rates in bacteria exceed phytoplankton production in unpductive aquatic systems, Nature, 385, 148–151, 1997. 8205

Goldman, J. C., Caron, D. A., and Dennett, M. R.: Regulation of gross growth efficiency and ammonium regeneration in bacteria by substrate C : N ratio, Limnol. Oceanogr., 32, 1239–1252, doi:10.4319/lo.1987.32.6.1239, 1987. 8213

Granskog, M. A., Stedmon, C. A., Dodd, P. A., Amon, R. M. W., Pavlov, A. K., De Steur, L., and Hansen, E.: Characteristics of colored dissolved organic matter (CDOM) in the Arctic outflow in the Fram Strait: assessing the changes and fate of terrigenous CDOM in the Arctic Ocean, J. Geophys. Res.-Oceans, 117, 1–13, doi:10.1029/2012JC008075, 2012. 8214

Hatzianastassiou, N., Matsoukas, C., Fotiadi, A., Pavlakis, K. G., Drakakis, E., Hatzidimitriou, D., and Vardavas, I.: Global distribution of Earth's surface shortwave radiation budget, Atmos. Chem. Phys., 5, 2847–2867, doi:10.5194/acp-5-2847-2005, 2005. 8208

Hobbie, J. E., Daley, R. J., and Jasper, S.: Use of nuclepore filters for counting bacteria by fluorescence microscopy. Use of nuclepore filters for counting bacteria by fluorescence microscopy, Appl. Environ. Microb., 33, 1225–1228, 1977. 8206

Jaffé, R., Ding, Y., Niggemann, J., Vähätalo, A. V., Stubbins, A., Spencer, R. G. M., Campbell, J., and Dittmar, T.: Global charcoal mobilization from soils via dissolution and riverine transport to the oceans, Science, 340, 345–347, doi:10.1126/science.1231476, 2013. 8203

Kester, D. R., Duedall, I. W., Connors, D. N., and Pytkowic, R.: Preparation of artificial seawater, Limnol. Oceanogr., 12, 176–179, doi:10.4319/lo.1967.12.1.0176, 1967. 8203

Title Page

Abstract | Introduction

Conclusions | References

Tables | Figures

◄ | ►

Back | Close

Full Screen / Esc

Printer-friendly Version

Interactive Discussion

Kieber, D. J. and Mopper, K.: Photochemical formation of glyoxylic and pyruvic acids in seawater, Mar. Chem., 21, 135–149, doi:10.1016/0304-4203(87)90034-X, 1987. 8215

Kieber, R. J., Zhou, X., and Mopper, K.: Formation of carbonyl compounds from UV-induced photodegradation of humic substances in natural waters: fate of riverine carbon in the sea, Limnol. Oceanogr., 35, 1503–1515, 1990. 8201, 8213, 8214

Koehler, B., Landelius, T., Weyhenmeyer, G. A., Machida, N., and Tranvik, L. J.: Sunlight-induced carbon dioxide emissions from inland waters, Global Biogeochem. Cy., 28, 696–711, doi:10.1002/2014GB004850, 2014. 8212

Kragh, T., Søndergaard, M., and Tranvik, L.: Effect of exposure to sunlight and phosphorus-limitation on bacterial degradation of coloured dissolved organic matter (CDOM) in freshwater, FEMS Microbiol. Ecol., 64, 230–9, doi:10.1111/j.1574-6941.2008.00449.x, 2008. 8216

Kroer, N.: Bacterial growth efficiency on natural dissolved organic matter, Limnol. Oceanogr., 38, 1282–1290, 1993. 8216

Lalonde, K., Vähätalo, A. V., and Gélinas, Y.: Revisiting the disappearance of terrestrial dissolved organic matter in the ocean: a δ^{13}C study, Biogeosciences, 11, 3707–3719, doi:10.5194/bg-11-3707-2014, 2014. 8203, 8204

Lønborg, C. and Álvarez Salgado, X. A.: Recycling versus export of bioavailable dissolved organic matter in the coastal ocean and efficiency of the continental shelf pump, Global Biogeochem. Cy., 26, 1–12, doi:10.1029/2012GB004353, 2012. 8200, 8204

Lønborg, C., Álvarez Salgado, X. A., Davidson, K., and Miller, A. E.: Production of bioavailable and refractory dissolved organic matter by coastal heterotrophic microbial populations, Estuar. Coast. Shelf S., 82, 682–688, doi:10.1016/j.ecss.2009.02.026, 2009. 8200

Massana, R., Gasol, J. M., Bjørnsen, P. K., Black-Burn, N., Hagström, Å., Hietanen, S., Hygum, B. H., Kuparinen, J., and Pedors-Alio, C.: Measurement of bacterial size via image analysis of epifluorescence preparations: description of an inexpensive system and solutions to some of the most common problems, Sci. Mar., 61, 397–407, 1997. 8206

Miller, W. L. and Moran, M. A.: Interaction of photochemical and microbial processes in the degradation of refractory dissolved organic matter from a coastal marine environment, Limnol. Oceanogr., 42, 1317–1324, available at: http://www.jstor.org/stable/10.2307/2839130, 1997. 8201, 8213, 8214

Miller, W. L. and Zepp, R. G.: Photochemical production of dissolved inorganic carbon from terrestrial organic matter: significance to the oceanic organic carbon cycle, Geophys. Res. Lett., 22, 417, doi:10.1029/94GL03344, 1995. 8217

Miller, W. L., Moran, M. A., and Sheldon, W. M.: Determination of apparent quantum yield spectra for the formation of biologically labile photoproducts, Limnol. Oceanogr., 47, 343–352, available at: http://www.jstor.org/stable/10.2307/3068981, 2002. 8201, 8211, 8212, 8215

Milliman, J. D. and Farnsworth, K. L.: River Discharge to the Coastal Ocean: a Global Synthesis, vol. 24, Cambridge University Press, Cambridge, doi:10.5670/oceanog.2011.108, 2011. 8203, 8230

Minor, E. C., Pothen, J., Dalzell, B. J., Abdulla, H., and Mopper, K.: Effects of salinity changes on the photodegradation and ultraviolet-visible absorbance of terrestrial dissolved organic matter, Limnol. Oceanogr., 51, 2181–2186, doi:10.4319/lo.2006.51.5.2181, 2006.

Moran, M. and Zepp, R.: Role of photoreactions in the formation of biologically labile compounds from dissolved organic matter, Limnol. Oceanogr., 42, 1307–1316, available at: http://www.aslo.org/lo/toc/vol_42/issue_6/1307.pdf, 1997. 8215

Nelson, N. B. and Siegel, D. A.: The global distribution and dynamics of chromophoric dissolved organic matter, Ann. Rev. Mar. Sci., 5, 447–76, doi:10.1146/annurev-marine-120710-100751, 2013. 8208, 8214

Norland, S.: The relationship between biomass and volume of bacteria, in: Handbook of Methods in Aquatic Microbial Ecology, edited by: Kemp, P., Sherr, B., Sherr, E., and Cole, J., Lewis Publishers, Boca Raton, 303–307, 1993. 8206

Obernosterer, I. and Herndl, G.: Differences in the optical and biological reactivity of the humic and nonhumic dissolved organic carbon component in two contrasting coastal marine environments, Limnol. Oceanogr., 45, 1120–1129, available at: http://www.jstor.org/stable/10.2307/2670702, 2000. 8201, 8213, 8214

Osburn, C. L., Zagarese, H. E., Morris, D. P., Hargreaves, B. R., and Cravero, W. E.: Calculation of spectral weighting functions for the solar photobleaching of chromophoric dissolved organic matter in temperate lakes, Limnol. Oceanogr., 46, 1455–1467, doi:10.4319/lo.2001.46.6.1455, 2001. 8217

R Core Team: R: a Language and Environment for Statistical Computing, R Foundation for Statistical Computing, Vienna, Austria, http://www.r-project.org/, 2014. 8205, 8209

Reader, H. E. and Miller, W. L.: The efficiency and spectral photon dose dependence of photochemically induced changes to the bioavailability of dissolved organic carbon, Limnol. Oceanogr., 59, 182–194, doi:10.4319/lo.2014.59.1.0182, 2014. 8201

Remington, S., Krusche, A., and Richey, J.: Effects of DOM photochemistry on bacterial metabolism and CO_2 evasion during falling water in a humic and a whitewater river in the

Brazilian Amazon, Biogeochemistry, 105, 185–200, doi:10.1007/s10533-010-9565-8, 2011. 8216

Rossel, P. E., Vähätalo, A. V., Witt, M., and Dittmar, T.: Molecular composition of dissolved organic matter from a wetland plant (*Juncus effusus*) after photochemical and microbial decomposition (1.25 yr): common features with deep sea dissolved organic matter, Org. Geochem., 60, 62–71, doi:10.1016/j.orggeochem.2013.04.013, 2013. 8215

Smith, E. and Benner, R.: Photochemical transformations of riverine dissolved organic matter: effects on estuarine bacterial metabolism and nutrient demand, Aquat. Microb. Ecol., 40, 37–50, doi:10.3354/ame040037, 2005. 8201, 8213

Smith, S. V. and Hollibaugh, J. T.: Coastal metabolism and the oceanic organic carbon balance, Rev. Geophys., 31, 75–89, 1993. 8201

Søndergaard, M. and Middelboe, M.: A cross-system analysis of labile dissolved organic carbon, Mar. Ecol.-Prog. Ser., 118, 283–294, available at: http://www.int-res.com/abstracts/meps/v118/p283-294/, 1995. 8200, 8201, 8204, 8205

Spencer, R. G. M., Aiken, G. R., Dornblaser, M. M., Butler, K. D., Holmes, R. M., Fiske, G., Mann, P. J., and Stubbins, A.: Chromophoric dissolved organic matter export from US rivers, Geophys. Res. Lett., 40, 1575–1579, doi:10.1002/grl.50357, 2013. 8208, 8214, 8230

Stedmon, C., Amon, R., Rinehart, A., and Walker, S.: The supply and characteristics of colored dissolved organic matter (CDOM) in the Arctic Ocean: pan arctic trends and differences, Mar. Chem., 124, 108–118, doi:10.1016/j.marchem.2010.12.007, 2011. 8208, 8214, 8230

Stepanauskas, R., Jørgensen, N. O. G., Eigaard, O. R., Zvikas, A., Tranvik, L. J., and Leonardson, L.: Summer inputs of riverine nutrients to the Baltic Sea: bioavailability and eutrophication relevance, Ecol. Monogr., 72, 579–597, 2002. 8206

Vähätalo, A. and Järvinen, M.: Photochemically produced bioavailable nitrogen from biologically recalcitrant dissolved organic matter stimulates production of a nitrogen-limited microbial food web in the Baltic Sea, Limnol. Oceanogr., 52, 132–143, 2007. 8201

Vähätalo, A. V.: Light, Photolytic Reactivity and Chemical Products – Encyclopedia of Inland Waters, vol. 2, 2nd edn., Likens, Oxford, doi:10.1016/B978-012370626-3.00110-1, 2009. 8215

Vähätalo, A. V. and Wetzel, R. G.: Photochemical and microbial decomposition of chromophoric dissolved organic matter during long (months–years) exposures, Mar. Chem., 89, 313–326, doi:10.1016/j.marchem.2004.03.010, 2004. 8217

Vähätalo, A. V., Aarnos, H., and Mäntyniemi, S.: Biodegradability continuum and biodegradation kinetics of natural organic matter described by the beta distribution, Biogeochemistry, 100, 227–240, doi:10.1007/s10533-010-9419-4, 2010. 8215, 8216

Vähätalo, A. V., Aarnos, H., Hoikkala, L., and Lignell, R.: Photochemical transformation of terrestrial dissolved organic matter supports hetero- and autotrophic production in coastal waters, Mar. Ecol.-Prog. Ser., 423, 1–14, doi:10.3354/meps09010, 2011. 8201, 8207, 8211, 8213

Warkentin, M., Freese, H. M., Karsten, U., and Schumann, R.: New and fast method to quantify respiration rates of bacterial and plankton communities in freshwater ecosystems by using optical oxygen sensor spots, Appl. Environ. Microb., 73, 6722–6729, doi:10.1128/AEM.00405-07, 2007. 8205

Warkentin, M., Freese, H. M., and Schumann, R.: Bacterial activity and bacterioplankton diversity in the eutrophic River Warnow – direct measurement of bacterial growth efficiency and its effect on carbon utilization, Microb. Ecol., 61, 190–200, doi:10.1007/s00248-010-9729-z, 2011. 8205

Wetzel, R. G., Hatcher, P. G., and Bianchi, T. S.: Natural photolysis by ultraviolet irradiance of recalcitrant dissolved organic matter to simple substrates for rapid bacterial metabolism, Limnol. Oceanogr., 40, 1369–1380, 1995. 8201

White, E. M., Kieber, D. J., Sherrard, J., Miller, W. L., and Mopper, K.: Carbon dioxide and carbon monoxide photoproduction quantum yields in the Delaware Estuary, Mar. Chem., 118, 11–21, doi:10.1016/j.marchem.2009.10.001, 2010.

Whitehead, R. F., de Mora, S., Demers, S., Gosselin, M., Monfort, P., and Mostajir, B.: Interactions of ultraviolet-B radiation, mixing, and biological activity on photobleaching of natural chromophoric dissolved organic matter: a mesocosm study, Limnol. Oceanogr., 45, 278–291, 2000. 8217

Wikner, J., Cuadros, R., and Jansson, M.: Differences in consumption of allochthonous DOC under limnic and estuarine conditions in a watershed, Aquat. Microb. Ecol., 17, 289–299, doi:10.3354/ame017289, 1999. 8216

Xiao, Y.-H., Sara-Aho, T., Hartikainen, H., and Vähätalo, A. V.: Contribution of ferric iron to light absorption by chromophoric dissolved organic matter, Limnol. Oceanogr., 58, 653–662, doi:10.4319/lo.2013.58.2.0653, 2013. 8203

Table 1. Locations and dates for sampling. City refers to a location close to the site of sampling given by coordinates. Transport time expresses the days elapsed between the sampling and the arrival of the sample to laboratory.

River	Location Country	City	Latitude	Longitude	Date Sampling	Transport time
Rio Negro[a]	Brazil	Manaus	03°07′59″ S	59°54′09″ W	3 Jun 2010	82
Rio Solimões[a]	Brazil	Manaus	03°07′58″ S	59°54′04″ W	3 Jun 2010	82
Congo	Congo	Kinshasa	04°18′18″ S	15°28′32″ E	1 May 2009	25
Danube	Romania	Tulcea	45°13′38″ N	28°44′50″ E	19 Apr 2010	21
Ganges–Brah.[b]	Bangladesh	Dhaka	23°34′12″ N	90°10′53″ E	1 Oct 2009	68
Lena	Russia	Tiksi	71°54′14″ N	127°15′16″ E	16 Aug 2009	155
Mekong	Kambodza	Phnom Penh	11°33′28″ N	104°56′53″ E	21 Aug 2009	34
Mississippi	USA	New Orleans	29°02′20″ N	89°19′20″ W	22 Apr 2009	34
Paraná	Argentina	Buenos Aires	34°18′07″ S	58°32′47″ W	29 Mar 2009	18
St. Lawrence	Canada	Quebec	46°54′45″ N	70°52′32″ W	12 Jun 2009	33
Yangtze	China	Shanghai	31°45′49″ N	121°2′22″ E	7 Sep 2009	17

[a] Amazon River sample was prepared by mixing samples from Rio Negro (25 %) and Rio Solimões (75 %).
[b] Ganges–Brahmaputra.

Table 2. Absorption coefficients of chromophoric dissolved organic matter at wavelength 300 nm ($a_{CDOM,300}$ m^{-1}) in the initial, the dark and the irradiated samples (mean ± sd of three determinations), the amount of photobleaching (Dark–Irradiated) given as absorption coefficient ($\Delta a_{CDOM,300}$ m^{-1}) as well as the relative difference (%) between the irradiated and to dark controls (Dark–Irradiated/Dark).

River	$a_{CDOM,300}$ Intial	Dark	Irradiated	Photobleaching $\Delta a_{CDOM,300}$	(Dark–Irradiated)/Dark (%)
Amazon	13.06 ± 0.03	12.92 ± 0.02	5.97 ± 0.02	6.95 ± 0.04	54 ± 0.1
Congo	21.61 ± 0.03	21.54 ± 0.03	9.12 ± 0.03	12.42 ± 0.06	58 ± 0.1
Danube	4.08 ± 0.03	3.79 ± 0.01	1.73 ± 0.02	2.06 ± 0.03	54 ± 0.4
Ganges–Brah.*	1.08 ± 0.03	1.12 ± 0.03	0.64 ± 0.03	0.48 ± 0.06	43 ± 1.1
Lena	10.92 ± 0.04	10.86 ± 0.02	5.22 ± 0.03	5.64 ± 0.05	52 ± 0.2
Mekong	2.41 ± 0.02	2.41 ± 0.01	1.21 ± 0.03	1.20 ± 0.04	50 ± 1.0
Mississippi	5.90 ± 0.05	6.01 ± 0.05	2.79 ± 0.04	3.22 ± 0.09	54 ± 0.3
Paraná	4.49 ± 0.08	4.48 ± 0.01	2.70 ± 0.01	1.78 ± 0.02	40 ± 0.1
St. Lawrence	6.39 ± 0.17	6.29 ± 0.07	3.12 ± 0.16	3.17 ± 0.23	50 ± 2.0
Yangtze	2.57 ± 0.05	2.63 ± 0.08	1.26 ± 0.03	1.37 ± 0.15	52 ± 0.3

* Ganges–Brahmaputra.

Full Screen / Esc

Printer-friendly Version

Interactive Discussion

Table 3. Bacterial cell densities (10^9 cells L^{-1}, mean ± sd of two replicates) in the beginning of bioassay ($t = 0$) and at the time of maximum cell density in the irradiated (Irradiated) samples and in the dark control samples (Dark), the time of maximal density (in days) and the relative increase in the density based on BLPs: (Irradiated–Dark)/Dark (%).

River	Cell density $t = 0$	Dark	Irradiated	Time of max density (d)	(Irradiated– Dark)/Dark (%)
Amazon	0.01	0.67 ± 0.02	1.54 ± 0.04	8	130 ± 01
Congo	0.03	1.89 ± 0.04	4.01 ± 0.12	5	112 ± 02
Danube	0.02	0.50 ± 0.02	1.04 ± 0.02	8	108 ± 04
Ganges–Brah.*	0.02	0.48 ± 0.03	0.73 ± 0.07	5	52 ± 05
Lena	0.03	0.36 ± 0.07	0.48 ± 0.04	6	33 ± 15
Mekong	0.02	0.64 ± 0.06	1.00 ± 0.04	12	56 ± 08
Mississippi	0.02	1.58 ± 0.03	2.53 ± 0.15	10	60 ± 06
Paraná	0.24	0.80 ± 0.03	1.09 ± 0.03	9	36 ± 01
St. Lawrence	0.03	0.59 ± 0.01	0.87 ± 0.00	12	47 ± 01
Yangtze	0.03	0.64 ± 0.06	1.08 ± 0.02	9	69 ± 13

* Ganges–Brahmaputra.

Table 4. Bacterial growth efficiency (%) (mean ± sd) on the irradiated DOC, the dark control DOC and on BLPs. BGE was calculated from BP (Fig. 1) and BR (Figs. 3 and 4). NA = not available.

River	BGE (%)		
	Irradiated	Dark	BLPs
Amazon	18.8 ± 0.7	15.3 ± 1.0	21.5 ± 2.0
Danube	12.8 ± 0.7	11.2 ± 0.1	15.5 ± 1.3
Ganges–Brah.*	27.7 ± 2.5	13.4 ± 1.7	NA
Lena	5.8 ± 0.1	9.9 ± 0.4	4.5 ± 0.9
Mekong	14.0 ± 0.2	12.5 ± 3.5	15.8 ± 4.5
St. Lawrence	13.2 ± 1.7	14.5 ± 2.1	12.0 ± 4.5
Yangtze	3.0 ± 0.2	3.6 ± 1.0	2.8 ± 1.1
Average	13.6 ± 8.1	11.5 ± 3.9	12.0 ± 7.2

* Ganges–Brahmaputra.

Table 5. The apparent quantum yields for the production of BLPs supporting bacterial production and respiration at 330 nm ($mol\,C\,mol\,absorbed\,photons^{-1}$), as well as the parameters c and d (nm^{-1}) for the calculation of spectral AQYs (Eq. 2).

River	BP			BR		
	$AQY_{BP,330}$	c	d	$AQY_{BR,330}$	c	d
Amazon	18.6	0.44	0.0305	56.5	0.57	0.0279
Congo	42.0	0.52	0.0286	–	–	–
Danube	35.9	0.49	0.0289	147.8	0.66	0.0255
Ganges–Brah.*	75.7	0.59	0.0271	–	–	–
Lena	9.9	0.37	0.0319	186.2	0.73	0.0251
Mekong	60.8	0.57	0.0277	269.6	0.78	0.0241
Mississippi	56.1	0.57	0.0280	–	–	–
Paraná	20.1	0.41	0.0301	–	–	–
St. Lawrence	9.5	0.37	0.0320	71.5	0.59	0.0273
Yangtze	36.2	0.49	0.0289	1203.6	1.03	0.0205

* Ganges–Brahmaputra.

Table 6. Calculated annual production of biologically labile photoproducts ($\mathrm{mmol\,C\,m^{-2}\,yr^{-1}}$) supporting bacterial production (BP on BLPs) and respiration (BR on BLPs) separately as well as their sum (BPLs). For these calculations, Eq. (3) received $\mathrm{AQY_{BP,\lambda}}$ or $\mathrm{AQY_{BR,\lambda}}$ from Table 5 and the spectral annual global radiation in the front of rivers examined.

River	BP on BLPs	BR on BLPs	BLPs
Amazon	8.1	27.8	35.9
Congo	20.0	–	–
Danube	9.4	46.7	56.1
Ganges–Brahmaputra	32.6	–	–
Lena*	1.0	25.8	26.8
Mekong	24.2	132.1	156.3
Mississippi	22.1	–	–
Paraná	6.4	–	–
St. Lawrence	2.0	18.9	20.9
Yangtze	10.2	573.8	584.0

"–" = Not determined.
* The attenuation of solar radiation by sea ice ignored.

V. Kasurinen et al.

Table 7. The absorption coefficient of CDOM at 300 nm, water discharge, CDOM and DOC fluxes, bacterial production (BP) and respiration (BR) based on BLPs, the total amount of BLPs and the fraction of BLPs from the DOC flux.

River	$a_{CDOM,300}$ [a] (m⁻¹)	discharge (km³ yr⁻¹)	CDOM flux (G m² yr⁻¹)	DOC flux (Mt C yr⁻¹)	BP based on BLPs (Mt C yr⁻¹)	BR based on BLPs (Mt C yr⁻¹)	BLPs (BP + BR) (Mt C yr⁻¹)	$\frac{BLPs}{DOC}$ (fraction)
Amazon	26.4	6300	166 320	37.5	0.67	5.58	6.25	0.17
Congo	49.4	1300	64 220	10.15	0.26	2.16	2.41	0.24
Danube	7.6	210	1596	0.59	0.01	0.05	0.06	0.10
Ganges–Brah.[b]	2.1	1120	2352	3.6	0.01	0.08	0.09	0.02
Lena	21.2	520	27 818	3.6	0.11	0.93	1.05	0.29
Mekong	5.1	550	2805	0.87	0.01	0.09	0.11	0.12
Mississippi	11.6	490	8800	3.5	0.04	0.30	0.34	0.09
Parana	8.4	530	4452	5.9	0.02	0.15	0.17	0.03
St. Lawrence	12	340	612	1.55	0.01	0.02	0.03	0.01
Yangtze	5	900	4500	1.8	0.02	0.15	0.17	0.09
Total		12 260	283 475	69.06	1.4	9.5	10.6	–
Mean	–	–	–	–	–	–	–	0.15

[a] $a_{CDOM,300}$ refers to the measured values from the water samples upon their arrival (Table 1), water discharge from Milliman and Farnsworth (2011), CDOM fluxes are calculated as the product of $a_{CDOM,300}$ and water discharges, but for Mississippi, St. Lawrence and Lena published CDOM fluxes were used (Stedmon et al., 2011; Spencer et al., 2013). DOC flux is from Cauwet (2002) but updated for Amazon (Coynel et al., 2005) and calculated for Mekong as the product of water discharge and DOC measured (1.58 mg L⁻¹) upon arrival of the Mekong sample, BP on BLPs is calculated from CDOM flux using the slope 0.333 mmol C m⁻² (Fig. 2), BR is calculated using BGE of 12.0 % on BLPs.
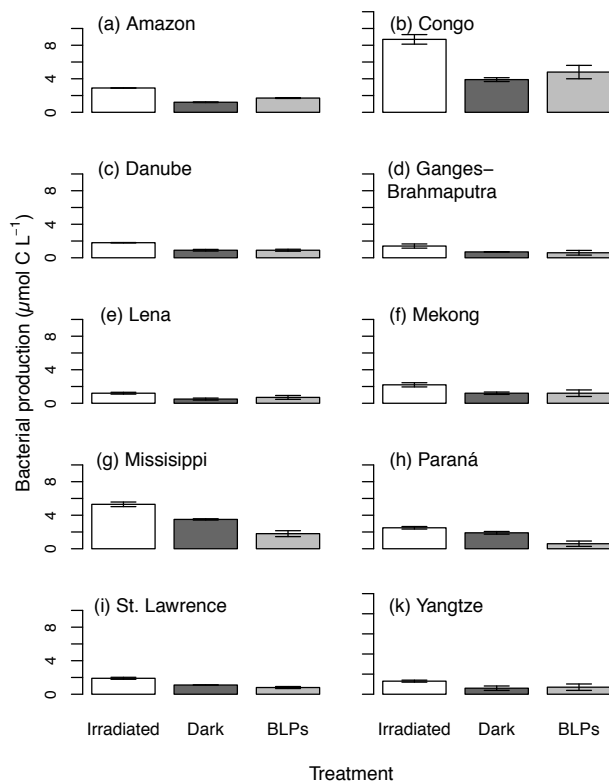[b] Ganges–Brahmaputra.

Figure 1. Bacterial production (µmol C L^{-1}; mean ± sd, $n = 2$) on the irradiated DOC (Irradiated), on the dark control DOC (Dark) and on BLPs, the latter calculated as the difference between the treatments (BLPs = Irradiated–Dark) by the end of logarithmic growth phase specified in Table 3.

Full Screen / Esc

Printer-friendly Version

Interactive Discussion
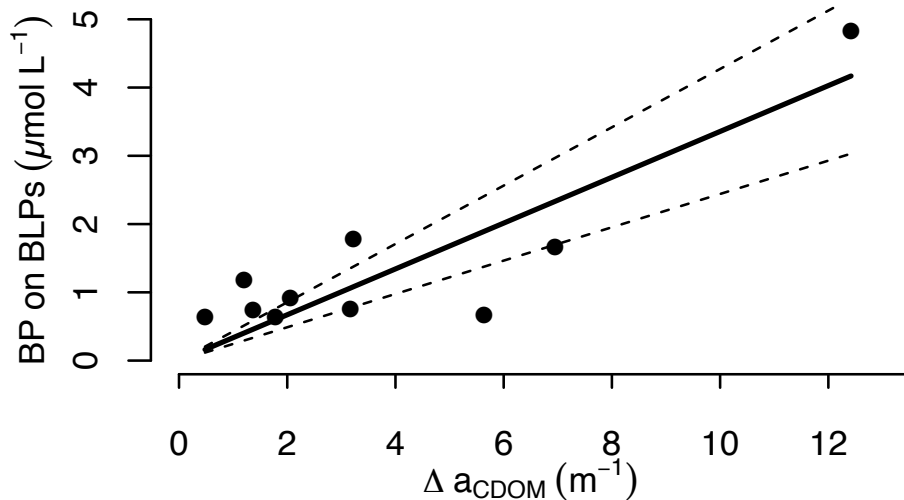
Figure 2. The relationship between the bacterial production based on biologically labile photo-products (BP on BLPs) and the photobleached CDOM at 300 nm. $\Delta a_{CDOM,300}$ shows individual samples, the solid line linear fit to the individual samples (BP on BLPs = $0.336 \, \Delta a_{CDOM,300}$; $R^2 = 0.871$, $F_{1,9} = 68.77$, df = 1,9, $p < 0.001$) and the dotted lines shows the 95 % confidence intervals of linear regression.
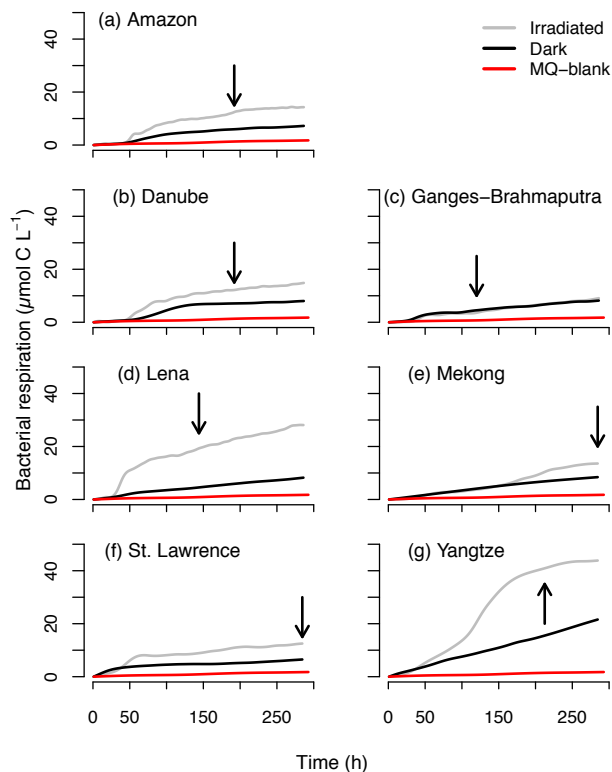
Figure 3. Cumulative bacterial respiration during the bioassay in the irradiated (gray line; Irradiated), and dark control samples (black line; Dark). Red line shows apparent respiration in the MQ-blank experiment (MQ-blank) and black arrows point out the end of log-phase in the irradiated samples (Table 3).
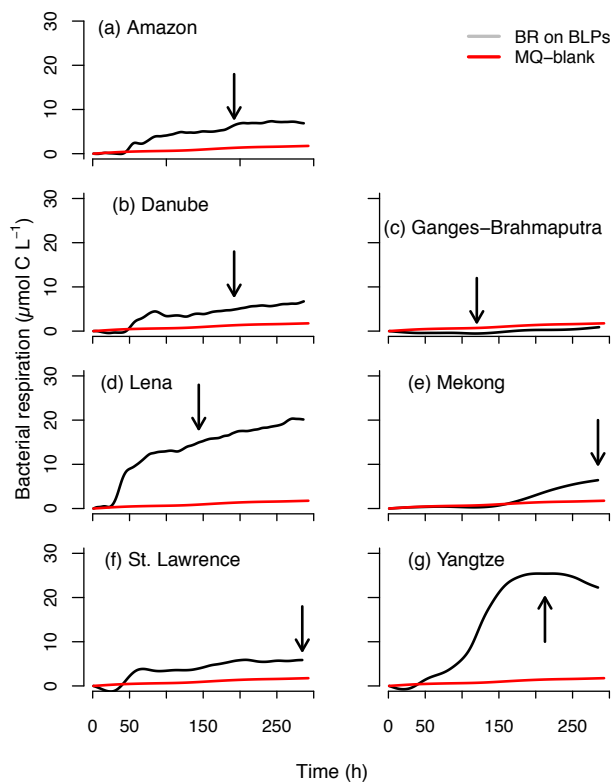
Figure 4. Cumulative bacterial respiration based on BLPs (BR on BLPs) calculated from Fig. 3 as the difference between irradiated and dark. Further details found in Fig. 3.

Title Page

Abstract | Introduction

Conclusions | References

Tables | Figures

|◀ | ▶|

◀ | ▶

Back | Close

Full Screen / Esc

Printer-friendly Version

Interactive Discussion